Quantitative Assays for Catalytic Photo-Oxygenation of Alzheimer Disease-Related Tau Proteins

Hiroki Umeda,[1] Taka Sawazaki,[3] Masahiro Furuta,[1] Takanobu Suzuki,[2] Shigehiro A. Kawashima,[1] Harunobu Mitsunuma,[1,4] Yukiko Hori,[2] Taisuke Tomita,[2] Youhei Sohma,[3] and Motomu Kanai[1,*]

[1]Laboratory of Synthetic Organic Chemistry, Graduate School of Pharmaceutical Sciences, The University of Tokyo, Tokyo 113-0033, Japan

[2]Laboratory of Neuropathology and Neuroscience, Graduate School of Pharmaceutical Sciences, The University of Tokyo, Tokyo 113-0033, Japan

[3]School of Pharmaceutical Sciences, Wakayama Medical University, Wakayama 640-8156, Japan

[4]JST, PRESTO, 4-1-8 Honcho, Kawaguchi, Saitama 332-0012, Japan.

KEYWORDS: Alzheimer Disease, tau, Photo-oxygenation

ABSTRACT: Catalytic photo-oxygenation of tau amyloid is a potential therapeutic approach to tauopathies, including Alzheimer disease (AD). However, tau is a complex target containing great molecular size and heterogeneous isoforms/proteoforms. Although catalytic photo-oxygenation has been confirmed when using catalyst **1** and recombinant tau pretreated with heparin, its effects on tau from human patients have not yet been clarified. In this study, focusing on the histidine residues being oxygenated, we have constructed two assay systems capable of quantitatively evaluating the catalytic activity when used on human patient tau: (1) fluorescence labeling at oxygenated histidine sites and (2) LC-MS/MS analysis of histidine-containing fragments. Using these assays, we identified **2** as a promising catalyst for oxygenation of human tau. In addition, our results suggest that aggregated tau induced by heparin is different from actual AD patient tau in developing effective photo-oxygenation catalysts.

Introduction

Alzheimer disease (AD) is a neurodegenerative disorder with cognitive decline and is the most common cause of dementia. AD is pathologically characterized by two types of lesions, senile plaques and neurofibrillary tangles, which are mainly composed of aggregated amyloid-β (Aβ) and tau, respectively.[1] Of these two, tangles have been reported to correlate more significantly with neuronal loss.[2] Moreover, there are known neurodegenerative diseases caused by tau accumulation, collectively known as tauopathies. Therefore, inhibition and clearance of aggregated tau may exhibit more direct therapeutic effects not only on AD but also tauopathies in general.

Aggregated Aβ as well as tau contains the cross-β-sheet structure and is called amyloid. Targeting the cross-β-sheet structure characteristic of amyloids, we developed Aβ amyloid-selective photo-oxygenation catalysts **1–4** (Figure 1a).[3-7] Only when interacting with the cross-β-sheet structure, do these catalysts act as photosensitizers to generate singlet oxygen ($^1O_2$) under light irradiation. Due to the short-lived nature of $^1O_2$,[8] it reacts selectively with the proximal Aβ amyloid. Specifically, histidine (His) was the main oxygenation site using catalysts **1–4**.[9] The covalent incorporation of hydrophilic oxygen atoms into the amyloid

decreased its aggregative property and facilitated phagocytotic degradation of Aβ amyloid by microglia cells in mice brains.[7]

Among those catalysts, BODIPY analog **1** photo-oxygenated the wild-type of the recombinant tau repeat domain (WTRD-tau) amyloid,[6,10] which is artificially aggregated with heparin.[1] Photo-oxygenation resulted in inhibition of its amyloid characteristics, such as cross-β-sheet propensity and seeding ability.[6,12] WTRD-tau is, however, a too-simplified model of tau derived from real AD patient (AD-tau) due to differences in molecular size [molecular weights (MW) of WTRD-tau and AD-tau are 13.4 kDa and 36.8~45.9 kDa, respectively] and complexity/heterogeneity. AD-tau is comprised of various isoforms and proteoforms containing post-translational modifications that play important roles in its function.[13] Also, the recent cryo-electron microscopy analysis revealed that the structures of protomer of WTRD-tau and AD-tau are distinct.[14] Hence, it is challenging but critically important to identify effective catalysts that oxygenate AD-tau through quantitative evaluation of the catalytic activity. Here we report two quantitative assay methods to evaluate oxygenation levels of AD-tau. These methods have allowed us to identify a promising catalyst **2** for AD-tau photo-oxygenation.

Results and discussion

Since protein oxygenation by singlet oxygen forms higher molecular-weight structures by crosslinking nucleophilic amino acid residues (e.g. His, Lys) and oxidatively generated electrophilic functional groups of His,[15] we initially attempted quantification of the crosslinked structures by Western blot (WB). However, WB of AD-tau showed complicated band patterns irrespective of photo-oxygenation (Figure 1b). Many high molecular-weight bands were observable with or without catalytic photo-oxygenation, showcasing the complexity/heterogeneity of AD-tau. It was difficult to identify the bands corresponding to crosslinked tau.
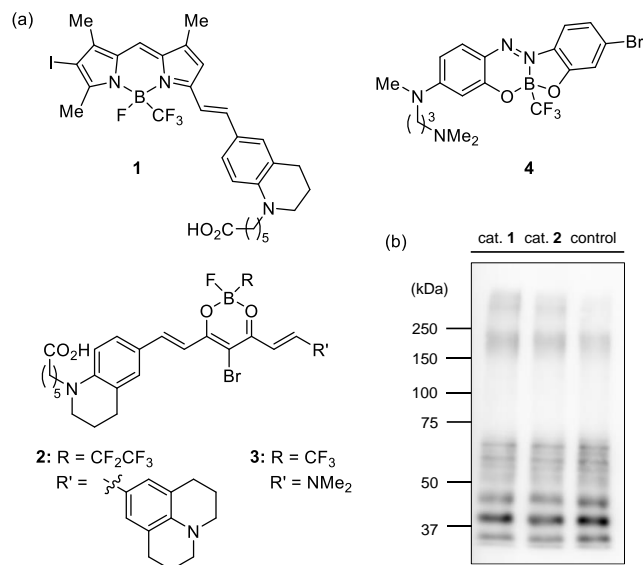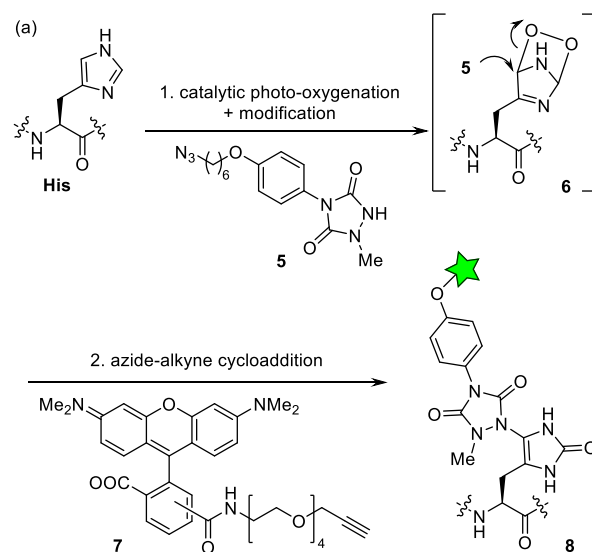

Figure 1. (a) Selective photo-oxygenation catalysts for Aβ (**1–4**) and WTRD-tau (**1**) amyloids. (b) Initial trial for quantification of oxygenated AD patient tau (AD-tau) by Western blot (WB). A mixture of the AD patient brain homogenate and catalyst (5 µM) was irradiated with 660 nm LED (3.0±0.5 mW/cm^2) at 37 °C for 100 min. WB was conducted using 5A6 tau antibody.

Considering that the main photo-oxygenation site of amyloids is His,[3] we envisioned quantifying photo-oxygenated His in tau with a fluorescent molecule. Sato et al. reported that a nucleophilic small molecule, 1-methyl-4-arylurazole (MAUra)-derivative **5**, selectively reacts with intermediate **6** generated through the reaction of His with $^1O_2$ (Figure 2a).[16,17] The modified sites can be further labeled with the fluorescent molecule, tetramethylrhodamine (TAMRA)-derivative **7**, through azide-alkyne cycloaddition (AAC) to afford **8** (Figure 2a).[18]

On the basis of this idea, we examined reaction conditions using catalyst **1** and the wild type of recombinant full-length 1N4R tau, one of the isoforms of human tau (Figure 2b, WTF-tau: MW = 43.0 kDa, 4 µM). After photo-oxygenation in the presence of **5** (400 µM) under irradiation of red LED light (λ_{max} = 660 nm) in phosphate-buffered saline (PBS) buffer, copper-promoted AAC was conducted with **7** (100 µM). The sodium dodecyl sulfate-polyacrylamide gel electrophoresis (SDS-PAGE) analysis with fluorescence

detection (λ_{ex} = 520 nm) showed the generation of fluorescent products **8** (Figure S4). The fluorescence of the bands in SDS-PAGE was significantly weaker under the control conditions without light irradiation, MAUra-derivative **5**, or AAC with fluorescent molecules **7**. The copper-catalyzed AAC was preferable to strain-promoted AAC (SPAAC)[19] using dibenzylcyclooctyne (DBCO)-PEG4-TAMRA, because the latter conditions showed nonspecific fluorescence labeling of tau unmodified with **5** (Figure S5). This fluorescence assay system is concise and well-behaved. The fluorescence intensity of the whole product solution, which corresponds to oxygenation yield, consistently increased with reaction time (Figure 2c, left) and amount of catalyst (Figure 2c, right). These results support the utility of this assay method for the quantitative evaluation of photo-oxygenation catalyst activity.

(b)
```
  1MAEPRQEFEV  MEDHAGTYGL  GDRKDQGGYT  MHQDQEGDTD  40
 41AGLKESPLQT  PTEDGSEEPG  SETSDAKSTP  TAEAEEEAGIG  80
 81DTPSLEDEAA  GHVTQARMVS  KSKDGTGSDD  KKAKGADGKT 120
121KIATPRGAAP  PGQKGQANAT  RIPAKTPPAP  KTPPSSGEPP 160
161KSGDRSGYSS  PGSPGTPGSR  SRTPSLPTPP  TREPKKVAVV 200
201RTPPKSPSSA  KSRLQTAPVP  MPDLKNVKSK  IGSTENLKHQ 240
241PGGGKVQIIN  KKLDLSNVQS  KCGSKDNIKH  VPGGGSVQIV 280
281YKPVDLSKVT  SKCGSLGNIH  HKPGGGQVEV  KSEKLDFKDR 320
321VQSKIGSLDN  ITHVPGGGNK  KIE  THKLTFR  ENAKAKTDHG 360
361AEIVYKSPVV  SGDTSPRHLS  NVSSTGSIDM  VDSPQLATLA 400
401DEVSASLAKQ  GL 412
```
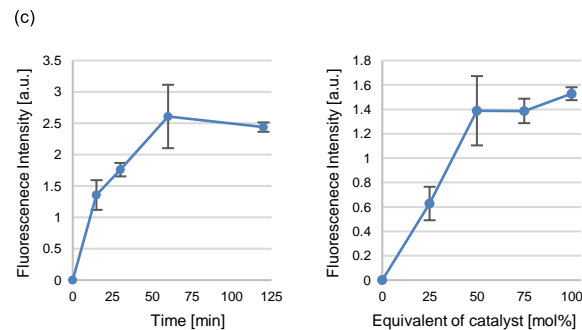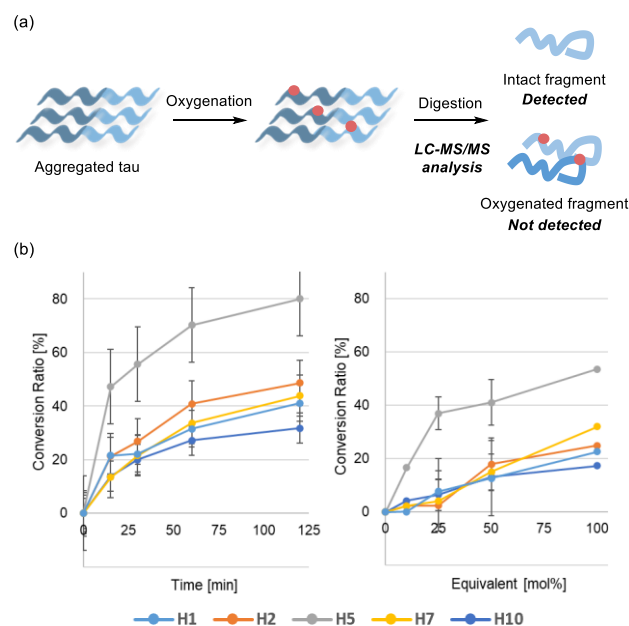
Figure 2. Quantitative evaluation of oxygenated tau by fluorescence assay. (a) A reaction scheme for quantitative evaluation of photo-oxygenated tau using two-step fluorescence labeling with MAUra technique. (b) Amino acid sequence of 1N4R tau (WTF-tau). The repeat domain corresponding to WTRD-tau are in bold letters. Fragments enzymatically digested with AspN/GluC to be detected by LC-MS/MS analysis are underlined (see Figure 3). (c) Time- and catalyst equivalent-dependencies of fluorescence intensity of **8**. Left: heparin-treated WTF-tau (4 μM), catalyst **1** (2 μM), and **5** (400 μM) were irradiated with 660 nm LED (3.0±0.5 mW/cm^2) in PBS buffer at 37 °C for a different reaction time, and then AAC was conducted with $CuSO_4$ (250 μM) and **7** (100 μM) to afford **8**. Error bars are based on three independent experiments. Right: heparin-treated WTF-tau (4 μM), a different equivalent of catalyst **1**, and **5** (400 μM) were irradiated with 660 nm LED in PBS buffer at 37 °C for 30 min, and then AAC was conducted with $CuSO_4$ (250 μM) and **7** (100 μM) to afford **8**. Data are averages of triple trials. Error bars indicate standard deviation.

To further validate the fluorescence assay, we next sought to establish a complementary assay method using mass spectrometry (MS).[20] After photo-oxygenation of WTF-tau (4 μM) with **1**, products were digested by AspN/GluC and the intensities of peptide fragments were quantified by LC-MS/MS analysis (Figure 3a). Because photo-oxygenation produced various products with different molecular weights by crosslinking, it was difficult to directly detect oxygenated fragments. Therefore, we quantified unreacted intact fragments. The catalytic activity was evaluated by determining the conversion ratio defined as $(1-R/T) \times 100[\%]$, where T (total) and R (remaining) are MS intensities of the fragments before and after photo-oxygenation, respectively.

The results showed that the conversion ratio of successfully detected fragments increased in both a time- (Figure 3b, left) and a catalyst concentration-dependent manner (Figure 3b, right), supporting the validity of this method. Furthermore, the reaction kinetics are consistent with those observed by the fluorescence method (Figure 2c). Intriguingly, the conversion ratio of the H5 fragment is greater than those of other fragments (See Figure 2b for the correspondence between fragment names and sequences). Given the presence of the H5 fragment in the cross-β-sheet structure of heparin-induced tau amyloid,[21] this observed tendency may reflect the cross-β-sheet selectivity of catalyst **1**.[6]

We next applied the two assay methods to compare the catalyst activities of **1**–**4** using a further advanced model of AD-tau, mice-expressed human 1N4R tau (MEH-tau, MW = 43.0 kDa).[22] MEH-tau harbors a familial frontotemporal dementia-linked P301S mutation and forms amyloid in mice brains. Therefore, MEH-tau extracted from mice brains is more relevant to AD-tau than WTF-tau, which requires heparin pretreatment. Whereas **3** was the most active catalyst for WTF-tau (Figure 4a), we determined that **2** was equally or more active than **3** for MEH-tau (Figure 4b). Because the amino acid sequence is identical between WTF-tau and MEH-tau except for the amino acid residue-301, the observed difference is likely due to the distinct conformations and/or aggregation states between these

two tau aggregates. Catalyst **2** can be activated with longer wavelength light (λ_{max} = 627 nm) than **3** (λ_{max} = 537 nm).[4] This property is favorable for *in vivo* applications because longer wavelength light is more cell- and tissue-permeable. Considering such favorable photophysical properties and catalyst activity, we selected **2** as the optimum photo-oxygenation catalyst for AD-tau.

Figure 3. Quantitative evaluation of oxygenated tau by LC-MS/MS. (a) LC-MS/MS analysis of enzyme-digested fragments of oxygenated tau. (b) Reaction time- (left) and catalyst equivalent-dependencies (right) of conversion ratios. Heparin-treated WTF-tau (4 μM) and **1** were irradiated with 660 nm LED (3.0±0.5 mW/cm^2) at 37 °C and the resulting mixture was digested with AspN/GluC in ammonium bicarbonate buffer for LC-MS/MS analysis. See Figure 2b for the correspondence between fragment names and sequences. Data are averages of triple trials. Error bars indicate standard deviation.

Finally, we compared the activity of catalyst **2** to **1**, the sole photo-oxygenation catalyst previously known to be active to tau (WTRD-tau),[10] using AD-tau prepared as a sarkosyl-insoluble fraction from an AD patient's brain. In the fluorescence assay, however, there was little difference in the fluorescence intensity between samples derived from an AD patient and a healthy person after photo-oxygenation (Figure S8). It may be due to the existence of only a very small concentration of AD-tau amyloid below the detection limit of the fluorescence assay in the samples. Using the LC-MS/MS method, however, we found that catalyst **2** was significantly more active than catalyst **1** (Figure S14, 8% vs. 0% conversion ratio using catalysts **2** and **1**, respectively). Notably, catalyst **1** showed little activity with AD-tau while it afforded >60% conversion ratio to WTF-tau (Figure 3b), supporting the idea that AD-tau amyloid furnishes completely distinct structures from artificially prepared WTRD-tau aggregates.[21,23] This is also supported by the fact that **1** was more active than **2** in the oxygenation of WTRD-tau.[6]
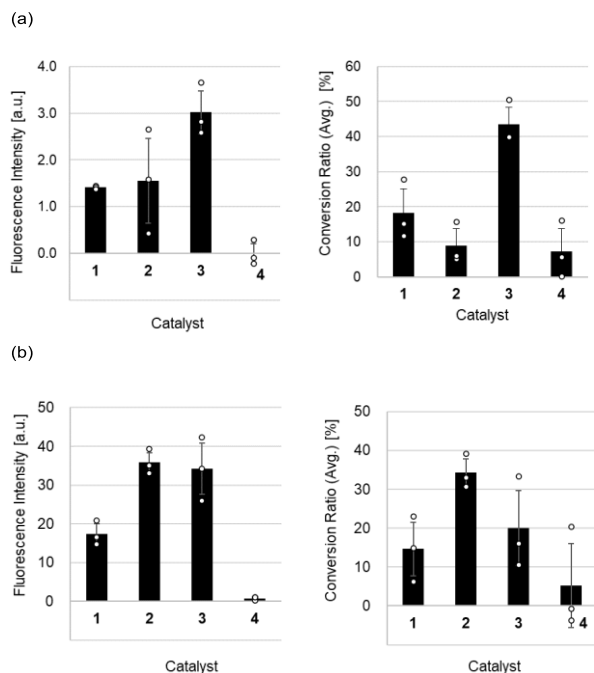
Figure 4. Comparison of catalyst activity of **1**–**4**. (a) Evaluation of catalytic activity using WTF-tau by fluorescence labeling (left) and LC-MS/MS analysis (right). A mixture of heparin-treated WTF-tau (4 µM) and catalyst (2 µM) was irradiated with 595 (for **3** and **4**)/660 nm (for **1** and **2**) LED (3.0±0.5 mW/cm²) at 37 °C for 30 min. The conversion ratio for LC-MS/MS analysis is the average of the conversion ratio for H1, H2, H5, H7, and H10. (b) Evaluation of catalytic activity using MEH-tau using fluorescence labeling (left) and LC-MS/MS analysis (right). A mixture of the sarkosyl-insoluble fractions from mouse brain homogenate containing MEH-tau and catalyst (1 µM) was irradiated with 595 nm LED for **3** and **4** and 660 nm LED for **1** and **2** (3.0±0.5 mW/cm²) at 37 °C for 30 min. The conversion ratio for LC-MS/MS analysis is the average of the conversion ratio for H1 and H7 fragments. Data are averages of triple trials. Error bars indicate standard deviation.

In summary, we developed two assay methods to quantify photo-oxygenation catalyst activity on full-length tau proteins, such as WTF-, MEH-, and AD-tau. The two methods, fluorescence and LC-MS/MS assays, were consistent with and complementary to each other. Although the fluorescence assay was not applicable to AD-tau due to the limited quantity of human AD patient sample available, LC-MS/MS assay was sufficiently sensitive. We identified **2** as the first photo-oxygenation catalyst applicable to AD-tau. Since catalyst **2** is excited by long-wavelength light and suited to animal experiments,[4] further structural modifications of **2** promise to produce clinically useful catalysts targeting tau amyloid.

Materials and Methods

General

All solvents and chemicals were purchased from commercial suppliers, Kanto Chemical Co., Inc., Sigma–Aldrich, Inc., Tokyo Chemical Industry Co., Ltd., Wako Pure Chemical Co., Inc., Watanabe Chemical Industries, Ltd., and Click Chemistry Tools, and were used without further purification. Nuclear magnetic resonance (NMR) spectra were recorded on JEOL ECX500 spectrometer, operating at 500 MHz for ^{1}H NMR and 124.51 MHz for ^{13}C NMR, or JEOL ECS400 spectrometer, operating at 400 MHz for ^{1}H NMR, 100 MHz for ^{13}C NMR, 369 MHz for ^{19}F NMR, and 126 MHz for ^{11}B NMR. Chemical shifts were reported in ppm on the δ scale relative to residual CHCl$_3$ (δ = 7.26 for ^{1}H NMR, δ =77.0 for ^{13}C NMR), and CD$_2$HCN (δ = 1.93 for ^{1}H NMR), DMSO-d_5 (δ = 39.5 for ^{13}C NMR), as an internal reference, and BF$_3$ (δ = 0.00 ppm for ^{11}B NMR) and hexafluorobenzene (δ = -164.90 ppm for ^{19}F NMR) as an external reference. For HRMS, ESI mass spectra were measured on a JEOL JMS-T100LC AccuTOF spectrometer, and APCI mass spectra were measured on a Bruker microTOF-II spectrometer. LC–MS/MS analyses were conducted using AB Sciex Triple TOF 4600 equipped with eksigent ekspert microLC 200, with a ChromXP C18 column (0.5 × 100 mm) using a linear gradient of 5–60% acetonitrile with 0.1% formic acid (v/v) in 0.1% aqueous formic acid (v/v) over 20 min at 40 °C with a flow rate of 20 µL/min. The eluent was monitored by on-line quadrupole time-of-flight mass spectrometer (ESI-Q-TOF MS), operated in positive ion mode. Data analysis was carried out on PeakView software (AB Sciex, version 1.2.0.3) based on the following method. Some of intense and/or characteristic MS/MS fragment ions were selected from each precursor ion, and chromatogram was extracted based on both the precursor and the fragment ions with a mass tolerance of 0.2 Da. Photoreaction was performed with a Valore light emitting diode (λ = 595 nm) and U-TECHNOLOGY light emitting diode (λ = 660 nm). Absorbance measurement was performed using a Shimadzu UV-1800 spectrometer with a rectangular quartz cell (5 mm pathlength). The fluorescence intensity was measured using Promega GloMax®.

Recombinant tau (WTF-tau) preparation

The human tau plasmid (2N4R full-length tau cloned into pRK172 vector) was gifted from Dr. Hasegawa.[24] The wild type of recombinant full-length 1N4R tau (WTF-tau) was constructed by deletion from full-length tau sequence.

Recombinant tau preparation was according to previous report of our group.[25] Briefly, wild-type tau protein was expressed in BL21(DE3) (Nippon Gene Co., Ltd.) and purified using the cation exchange chromatography column with cellulose phosphate. After elution, the eluates were applied to reverse-phase chromatography to increasing the purity. After the evaporating of elution buffer from reverse-phase chromatography, the pellets were dissolved with phosphate buffered saline (PBS), the concentration of tau was measured by BCA assay kit (Takara), and the resulting tau solution was stocked at -30 °C until use.

Heparin induced WTF-tau aggregation

To a solution of WTF-tau (4 µM) in PBS buffer, 1,4-dithiothreitol (DTT: 2 mM) and heparin-sodium (4 µM) were added. The mixture was incubated at 37 °C for 24 hrs. The mixture was stocked at -80°C until use.

Mouse brain samples (MEH-tau)

All experiments using animals were performed according to the guidelines provided by the Institutional Animal Care Committee of the Graduate School of Pharmaceutical Sciences at the

University of Tokyo (protocol no.: P31-11). PS19 mice, which are human tau transgenic mice with age-dependent deposition of human 1N4R tau with P301S mutation, were used as Alzheimer disease mouse models. Wild-type animals were 8-week-old C57BL/6J mice (Japan SLC, Inc). All animals were maintained on a 12 h light/dark cycle with food and water available ad libitum.

Human brain samples (AD-tau)

Samples of brain tissue from patients with Alzheimer disease and aged controls were obtained from the tissue bank at the University of Pennsylvania Alzheimer's Disease Core Center (ADCC) and the Center for Neurodegenerative Disease Research (CNDR). Alzheimer's disease and control patients were diagnosed symptomatically and pathologically at ADCC-CNDR as previously described.[26] All samples used in experiments were obtained from temporal cortex under the approval of the institutional review board, ADCC-CNDR, and the institutional ethical committee of the Graduate School of Pharmaceutical Sciences, University of Tokyo (No. 2-1).

Sarkosyl insoluble fraction (SIF) preparation

A whole brain from PS19 mouse or a piece of the brain tissue from AD patient was homogenized in PBS buffer containing cOmplete and phosSTOP, and then subjected to sonication. The solution was ultra-centrifuged at 113,000 x g, 4 °C for 20 min. The pellet was sonicated again to afford SIF suspension solution.

Western blotting of human brain samples

After sonication of the brain tissue from an AD patient in PBS buffer containing cOmplete and phosSTOP at output 1.5 for 10-20 sec, the mixture of the homogenate and catalyst (5 μM) was irradiated with 660 nm LED (3.0±0.5 mW/cm^2) at 37 °C for 100 min. The samples were separated by SDS-PAGE, and western blotting was conducted using anti tau antibody (5A6).

Fluorescent labeling assay

To a solution of WTF-tau aggregates (4 μM) or a sarkosyl insoluble fraction (SIF), a stock solution of catalyst **1-4** (2 μM in WTF-tau, 1uM in SIF) and azide conjugated MAUra **5** (400 μM) were added. The mixture was irradiated with 595 nm (for catalyst **3** or **4**) or 660 nm (for catalyst **1** or **2**) LED (suitable for catalyst absorption wavelength) at 37 °C for 30 min, and then subjected to acetone precipitation after addition of coumarin-conjugated HaloTag protein as internal standard. To the pellet was added SDS sample buffer (without dithiothreitol (DTT) and bromophenol blue (BPB)), and then the mixture was boiled at 95 °C for 5 min. To the solution, TBTA (500 μM), CuSO$_4$ (250 μM), alkyne conjugated TAMRA **7** (100 μM), and L(+)-ascorbic acid sodium salt (2 mM) were added and then the mixture was incubated at room temperature for 1 hr. The solution was again subjected to acetone precipitation. The pellet was dissolved in SDS sample buffer (without BPB), and the mixture was boiled at 95 °C for 5 min. The fluorescence intensity of the solution was analyzed in duplicate using GloMax® (λ_{ex} = 365 nm for coumarin / 520 nm for TAMRA). The fluorescence intensity for evaluation was provided as the fluorescence intensity of TAMRA divided by the fluorescence intensity of coumarin. The fluorescence intensity of a sample without oxygenation was subtracted as a background from that of samples with oxygenation. In the WTF-tau sample, Hela cell extract was added after the photo-oxygenation reaction to promote pellet formation in acetone precipitation.

LC-MS/MS analysis assay

To a solution of WTF-tau aggregates (4 μM) or a sarkosyl insoluble fraction (SIF), a stock solution of catalyst **1-4** (2 μM in WIF-tau, 1 uM in SIF) was added. The mixture was irradiated 595 nm (for catalyst **3** or **4**) or 660 nm (for catalyst **1** or **2**) LED (suitable for catalyst absorption wavelength) at 37 °C for 30 min, and then subjected to sonication with urea (8 M) and DTT (10 mM). The solvent was exchanged to ammonium bicarbonate aqueous solution (50 mM) with Amicon Ultra, and then enzymatically digested with AspN/GluC at 37 °C for 3-18 hrs. The solvent was exchanged to sample buffer (5% formic acid, 5% acetonitrile in water), and then fragments were analyzed in duplicate using LC-MS/MS. The quantified peak areas were converted to relative values using a His- and Met-free fragment, as internal standards (fragment IS), which is not to be oxygenated. Considering the fragment area of the sample without oxygenation (T; Total) as 100% of the raw material, the fragment area of the sample with oxygenation (R; Remain) was also converted to conversion ratio through the formula (1).

$$\frac{T - R}{T} \times 100 \quad [\%] \qquad (\mathbf{1})$$

Associated content

Supporting Information

The Supporting Information is available free of charge on the ACS Publications website. Synthetic protocols and Figure S1-S14 (PDF).

Author information

Corresponding Author

Motomu Kanai – Laboratory of Synthetic Organic Chemistry, Graduate School of Pharmaceutical Sciences, The University of Tokyo, 7-3-1 Hongo, Bunkyo-ku, Tokyo, 113-0033, Japan; orcid.org/0000-0003-1977-7648; Email: kanai@mol.f.u-tokyo.ac.jp

Authors

Hiroki Umeda – Laboratory of Synthetic Organic Chemistry, Graduate School of Pharmaceutical Sciences, The University of Tokyo, 7-3-1 Hongo, Bunkyo-ku, Tokyo, 113-0033, Japan
Taka Sawazaki – School of Pharmaceutical Sciences, Wakayama Medical University, Wakayama 640-8156, Japan
Masahiro Furuta – Laboratory of Synthetic Organic Chemistry, Graduate School of Pharmaceutical Sciences, The University of Tokyo, 7-3-1 Hongo, Bunkyo-ku, Tokyo, 113-0033, Japan
Takanobu Suzuki – Laboratory of Neuropathology and Neuroscience, Graduate School of Pharmaceutical Sciences, The University of Tokyo, 7-3-1 Hongo, Bunkyo-ku, Tokyo, 113-0033, Japan
Shigehiro A. Kawashima – Laboratory of Synthetic Organic Chemistry, Graduate School of Pharmaceutical Sciences, The University of Tokyo, 7-3-1 Hongo, Bunkyo-ku, Tokyo, 113-0033, Japan
Harunobu Mitsunuma – Laboratory of Synthetic Organic Chemistry, Graduate School of Pharmaceutical Sciences, The University of Tokyo, 7-3-1 Hongo, Bunkyo-ku, Tokyo, 113-0033,

Japan and JST, PRESTO, 4-1-8 Honcho, Kawaguchi, Saitama 332-0012, Japan

Yukiko Hori – Laboratory of Neuropathology and Neuroscience, Graduate School of Pharmaceutical Sciences, The University of Tokyo, 7-3-1 Hongo, Bunkyo-ku, Tokyo, 113-0033, Japan

Taisuke Tomita – Laboratory of Neuropathology and Neuroscience, Graduate School of Pharmaceutical Sciences, The University of Tokyo, 7-3-1 Hongo, Bunkyo-ku, Tokyo, 113-0033, Japan

Youhei Sohma – School of Pharmaceutical Sciences, Wakayama Medical University, Wakayama 640-8156, Japan

Notes

Acknowledgment

References

(1) Knopman, D. S.; Amieva, H.; Petersen, R. C.; Chételat, G.; Holtzman, D. M.; Hyman, B. T.; Nixon, R. A.; Jones, D. T. Alzheimer disease. *Nat. Rev. Dis. Primers.* **2021**, *7*, 33.

(2) Gómez-Isla, T.; Hollister, R.; West, H.; Mui, S.; Growdon, J. H.; Petersen, R. C.; Parisi, J. E.; Hyman, B. T. Neuronal loss correlates with but exceeds neurofibrillary tangles in Alzheimer's disease. *Annals. of Neurology.* **1997**, *41*, 17-24.

(3) (a) Sohma, Y.; Sawazaki, T.; Kanai, M. Chemical catalyst-promoted photooxygenation of amyloid proteins. *Org. Biomol. Chem.* **2021**, *19*, 10017-10029. (b) Tomizawa, I.; Nakagawa, H.; Sohma, Y.; Kanai, M.; Hori, Y.; Tomita, T. Photo-Oxygenation as a New Therapeutic Strategy for Neurodegenerative Proteinopathies by Enhancing the Clearance of Amyloid Proteins. *Front Aging Neurosci.* **2022**, *14*, 945017.

(4) Ni, J.; Taniguchi, A.; Ozawa, S.; Hori, Y.; Kuninobu, Y.; Saito, T.; Saido, T. C.; Tomita, T.; Sohma, Y.; Kanai. M. Near-Infrared Photoactivatable Oxygenation Catalysts of Amyloid Peptide. *Chem* **2018**, *4*, 807-820.

(5) Nagashima, N.; Ozawa, S.; Furuta, M.; Oi, M.; Hori, Y.; Tomita, T.; Sohma, Y.; Kanai, M. Catalytic photooxygenation degrades brain Aβ in vivo. *Sci. Adv.* **2021**, *7*, No. eabc9750.

(6) Suzuki, T.; Hori, Y.; Sawazaki, T.; Shimizu, Y.; Nemoto, Y.; Taniguchi, A.; Ozawa, S.; Sohma, Y.; Kanai, M.; Tomita, T. Photo-oxygenation inhibits tau amyloid formation. *Chem. Commun.* **2019**, *55*, 6165-6168.

(7) Ozawa, S.; Hori, Y.; Shimizu, Y.; Taniguchi, A.; Suzuki, T.; Wang, W.; Chiu, Y. W.; Koike, R.; Yokoshima, S.; Fukuyama, T.; Takatori, S.; Sohma, Y.; Kanai, M.; Tomita, T. Photo-oxygenation by a biocompatible catalyst reduces amyloid-β levels in Alzheimer's disease mice. *Brain* **2021**, *144*, 1884-1897.

(8) Ogilby, P. R. Singlet oxygen: there is indeed something new under the sun. *Chem. Soc. Rev.* **2010**, *39*, 3181-3209.

(9) Grassi, L.; Cabrele, C. Susceptibility of protein therapeutics to spontaneous chemical modifications by oxidation, cyclization, and elimination reactions. *Amino Acids.* **2019**, *51*, 1409-1431.

(10) (a) Crowther, R. A.; Olesen, O. F.; Jakes, R.; Goedert, M. The microtubule binding repeats of tau protein assemble into filaments like those found in Alzheimer's disease. *FEBS Letters.* **1992**, *309*, 199-202. (b) Wille, H.; Drewes, G.; Biernat, J.; Mandelkow, E. M.; Mandelkow, E. Alzheimer-like paired helical filaments and antiparallel dimers formed from microtubule-associated protein tau in vitro. *J. Cell. Biol.* **1992**, *118*, 573-584.

(11) (a) Pérez, M.; Valpuesta, J. M.; Medina, M.; de Garcini, E. M.; Avila, J. Polymerization of τ into Filaments in the Presence of Heparin: The Minimal Sequence Required for τ - τ Interaction. *J. Neurochem.* **1996**, 67, 1183-1190. (b) Goedert, M.; Jakes, R.; Spillantini, M. G.; Hasegawa, M.; Smith, M. J.; Crowther, R. A. Assembly of microtubule-associated protein tau into Alzheimer-like filaments induced by sulphated glycosaminoglycans. *Nature* **1996**, *383,* 550-553.

(12) For a precedent of non-selective catalytic photo-oxygenation of tau, see; Dubey, T.; Gorantla, N. V.; Chandrashekara, K. T.; Chinnathambi, S. Photoexcited Toluidine Blue Inhibits Tau Aggregation in Alzheimer's Disease. *ACS Omega* **2019**, *4*, 18793–18802.

(13) (a) Wesseling, H.; Mair, W.; Kumar, M.; Schlaffner, C. N.; Tang, S.; Beerepoot, P.; Fatou, B.; Guise, A. J.; Cheng, L.; Takeda, S.; Muntel, J.; Rotunno, M. S.; Dujardin, S.; Davies, P.; Kosik, K. S.; Miller, B. L.; Berretta, S.; Hedreen, J. C.; Grinberg, L. T.; Seeley, W. W.; Hyman, B. T.; Steen, H.; Steen, J. A. Tau PTM Profiles Identify Patient Heterogeneity and Stages of Alzheimer's Disease. *Cell* **2020**, *183*, 1699-1713. (b) Alquezar, C.; Arya, S.; Kao, A. W. Tau Post-translational Modifications: Dynamic Transformers of Tau Function, Degradation, and Aggregation. *Front. Neurol.* **2021**, 11, 595532.

(14) Shi, Y.; Zhang, W.; Yang, Y.; Murzin, A. G.; Falcon, B.; Kotecha, A.; Beers, M.; Tarutani, A.; Kametani, F.; Garringer, H. J.; Vidal, R.; Hallinan, G. I.; Lashley, T.; Saito, Y.; Murayama, S.; Yoshida, M.; Tanaka, H.; Kakita, A.; Ikeuchi, T.; Robinson, A. C.; Mann, D. M. A.; Kovacs, G. G.; Revesz, T.; Ghetti, B.; Hasegawa, M.; Goedert M.; ScheresStructure-based classification of tauopathies. *Nature* **2021**, *598*, 359-363.

(15) (a) Xu, C.; Chen, Y.; Yi, L.; Brantley, T.; Stanley, B.; Sosic, Z.; Zang, L. Discovery and Characterization of Histidine Oxidation Initiated Cross-links in an IgG1 Monoclonal Antibody. *Anal. Chem.* **2017**, *89*, 7915-7923. (b) Leshem, G.; Richman, M.; Lisniansky, E.; Antman-Passig, M.; Habashi, M.; Gräslund, A.; Wärmländer, S. K. T. S.; Rahimipour, S. Photoactive chlorin e6 is a multifunctional modulator of amyloid-β aggregation and toxicity via specific interactions with its histidine residues. *Chem. Sci.* **2019**, *10*, 208-217. (c) Powell, T.; Knight, M. J.; Wood, A.; O'Hara, J.; Burkitt, W. Photoinduced cross-linking of formulation buffer amino acids to monoclonal antibodies. *Biopharmaceutics* **2021**, *160*, 35-41.

(16) (a) Nakane, K.; Sato, S.; Niwa, T.; Tsushima, M.; Tomoshige, S.; Taguchi, H.; Ishikawa, M.; Nakamura, H. Proximity Histidine Labeling by Umpolung Strategy Using Singlet Oxygen. *J. Am. Chem. Soc.* **2021**, *143*, 7726-7731. (b) Nakane, K.; Niwa, T.; Tsushima, M.; Tomoshige, S.; Taguchi, H.; Nakamura, H.; Ishikawa, M.; Sata, S. BODIPY Catalyzes Proximity-Dependent Histidine Labelling. *Chem. Cat. Chem.* **2022**, *14*, No. e202200077. (c) Nakane, K.; Nagasawa, H.; Fujimura, C.; Koyanagi, E.; Tomoshige, S.; Ishikawa, M.; Sato, S. Switching of Photocatalytic Tyrosine/Histidine Labeling and Application to Photocatalytic Proximity Labeling. *Int. J. Mol. Sci.* **2022**, *23*, 11622.

(17) For other labeling methods of oxygenated histidine residue, see; (a) Müller, M.; Gräbnitz, F.; Barandun, N.; Shen, Y.; Wendt, F.; Steiner, S. N.; Severin, Y.; Vetterli, S. U.; Mondal, M.; Prudent, J. R.; Hofmann, R.; Oostrum, M.; Sarott, R. C.; Nesvizhskii, A. I.; Carreira, E. M.; Bode, J. W.; Snijder, B.; Robinson, J. A.; Loessner, M. J.; Oxenius, A.; Wollscheid, B. Light-mediated discovery of surfaceome nanoscale organization and intercellular receptor interaction networks. *Nat. Commun.* **2021**, *12*, 7036. (b) Wang, H.; Wang, Z.; Gao, H.; Liu, J.; Qiao, Z.; Zhao, B.; Liang, Z.; Jiang, B.; Zhang, L.; Zhang, Y. A

photo-oxidation driven proximity labeling strategy enables profiling of mitochondrial proteome dynamics in living cells. *Chem. Sci.* **2022**, *13*, 11943-11950.

(18) For reviews on azide-alkyne cycloaddition, see; (a) Kolb, H. C.; Finn, M. G.; Sharpless, K. B. *Angew. Chem. Int. Ed.* **2001**, *40*, 2004-2021. (b) Meldal, M.; Tomoe, C. W. Cu-Catalyzed Azide-Alkyne Cycloaddition. *Chem. Rev.* **2008**, *108*, 2952-3015. (c) Jewett, J. C.; Bertozzi, C. R. Cu-free click cycloaddition reactions in chemical biology. *Chem. Soc. Rev.* **2010**, *39*, 1272-1279.

(19) Agard, N. J.; Prescher, J. A.; Bertozzi, C. A. A Strain-Promoted [3 + 2] Azide–Alkyne Cycloaddition for Covalent Modification of Biomolecules in Living Systems. *J. Am. Chem. Soc.* **2004**, *126*, 15046-15047.

(20) For quantification of post translational modifications of tau, see; (a) Mair, W.; Muntel, J.; Tepper, K.; Tang, S.; Biernat, J.; Seeley, W. W.; Kosik, K. S.; Mandelkow, E.; Steen, H.; Steen, J. A. FLEXITau: Quantifying Post-translational Modifications of Tau Protein in Vitro and in Human Disease. *Anal. Chem.* **2016**, *88*, 3704-3714. (b) Zhou, M.; Duong, D. M.; Johnson, E. C. B.; Dai, J.; Lah, J. J.; Levey, A. I. Seyfried, N. T. Mass Spectrometry-Based Quantification of Tau in Human Cerebrospinal Fluid Using a Complementary Tryptic Peptide Standard. *J. Proteome Res.* **2019**, *18*, 2422-2432.

(21) Zhang, W.; Falcon, B.; Murzin, A. G.; Fan, J.; Crowther, R. A.; Goedert, M.; Scheres, S. H. Heparin-induced tau filaments are polymorphic and differ from those in Alzheimer's and Pick's disease. *eLife* **2019**, *8*, No. e43584.

(22) Yoshiyama, Y.; Higuchi, M.; Zhang, B.; Huang, S.; Iwata, N.; Saido, T. C.; Maeda, J.; Suhara, T.; Trojanowski, J. Q.; Lee, V. M. Synapse loss and microglial activation precede tangles in a P301S tauopathy mouse model. *Neuron* **2007**, *53*, 337-351.

(23) Fichou, Y.; Vigers, M.; Goring, A. K.; Eschmann, N. A.; Han, S. Heparin-induced tau filaments are structurally heterogeneous and differ from Alzheimer's disease filaments. *Chem. Commun.* **2018**, *54*, 4573-4576.

(24) Takahashi, M.; Miyata, H.; Kametani, F.; Nonaka, T.; Akiyama, H.; Hisanaga, S. and Hasegawa, M. Extracellular association of APP and tau fibrils induces intracellular aggregate formation of tau. *Acta Neuropathol.*, **2015**, 129, 895-907.

(25) Goedert, M. and Jakes, R. Expression of separate isoforms of human tau protein: correlation with the tau pattern in brain and effects on tubulin polymerization. *EMBO J.*, **1990**, 9, 4225-42304.

(26) Arnold, S. E.; Lee, E. B.; Moberg, P. J.; Stutzbach, L.; Kazi, H.; Han, L.; Lee, V. M. Y. and Trojanowski, J. Q. Olfactory epithelium amyloid-beta and paired helical filament-tau pathology in Alzheimer disease. *Ann. Neurol.* **2010**, 67, 462-469.